



## Annual greenhouse gas budget for a bog ecosystem undergoing restoration by rewetting

Sung-Ching Lee<sup>1</sup>, Andreas Christen<sup>1</sup>, Andy T. Black<sup>2</sup>, Mark S. Johnson<sup>3,4</sup>, Rachhpal S. Jassal<sup>2</sup>, Rick Ketler<sup>1</sup>, Zoran Nestic<sup>1,2</sup>, Markus Merkens<sup>5</sup>

5 <sup>1</sup>Department of Geography / Atmospheric Science Program, The University of British Columbia, Vancouver, Canada

<sup>2</sup>Faculty of Land and Food Systems, The University of British Columbia, Vancouver, Canada

<sup>3</sup>Institute of Resources, Environment and Sustainability, The University of British Columbia, Vancouver, Canada

<sup>4</sup>Department of Earth, Ocean and Atmospheric Sciences, The University of British Columbia, Vancouver, Canada

<sup>5</sup>Parks, Planning and Environment Department, Metro Vancouver, Vancouver, Canada

10

Correspondence to: S.-C. Lee (sungching.lee@geog.ubc.ca)

**Abstract.** Many peatlands have been drained and harvested for peat mining, which has turned them from carbon (C) sinks into C emitters. Rewetting of disturbed peatlands facilitates their ecological recovery, and may help them revert to carbon dioxide (CO<sub>2</sub>) sinks. However, rewetting may also cause substantial emissions of the more potent greenhouse gas (GHG) methane (CH<sub>4</sub>). Our knowledge on the exchange of CO<sub>2</sub> and CH<sub>4</sub> following rewetting during restoration of disturbed peatlands is currently limited. This study quantifies annual fluxes of CO<sub>2</sub> and CH<sub>4</sub> in a disturbed and rewetted area located in the Burns Bog Ecological Conservancy Area in Delta, BC, Canada. Burns Bog is recognized as the largest raised bog ecosystem on North America's West Coast. Burns Bog was substantially reduced in size and degraded by peat mining and agriculture. Since 2005, the bog has been declared a conservancy area, with restoration efforts focusing on rewetting disturbed ecosystems to recover *Sphagnum* and suppress fires. Using the eddy-covariance (EC) technique, we measured year-round (16<sup>th</sup> June 2015 to 15<sup>th</sup> June 2016) turbulent fluxes of CO<sub>2</sub> and CH<sub>4</sub> from a tower platform in an area rewetted for the last 8 years. The study area, dominated by sedges and *Sphagnum*, experienced a varying water table position that ranged between 7.7 (inundation) and -26.5 cm from the surface during the study year. The annual CO<sub>2</sub> budget of the rewetted area was -179 g CO<sub>2</sub>-C m<sup>-2</sup> year<sup>-1</sup> (CO<sub>2</sub> sink) and the annual CH<sub>4</sub> budget was 16 g CH<sub>4</sub>-C m<sup>-2</sup> year<sup>-1</sup> (CH<sub>4</sub> source). Gross ecosystem productivity (GEP) exceeded ecosystem respiration (*R<sub>e</sub>*) during summer months (June-August), causing a net CO<sub>2</sub> uptake. In summer, high CH<sub>4</sub> emissions (121 mg CH<sub>4</sub>-C m<sup>-2</sup> day<sup>-1</sup>) were measured. In winter (December-February), while roughly equal magnitudes of GEP and *R<sub>e</sub>* made the study area CO<sub>2</sub> neutral, very low CH<sub>4</sub> emissions (9 mg CH<sub>4</sub>-C m<sup>-2</sup> day<sup>-1</sup>) were observed. The key environmental factors controlling the seasonality of these exchanges were downwelling photosynthetically active radiation and 5-cm soil temperature. It appears that the high water table caused by ditch blocking which suppresses *R<sub>e</sub>*. With low temperatures in winter, CH<sub>4</sub> emission was more suppressed than *R<sub>e</sub>*. Annual net GHG flux from CO<sub>2</sub> and CH<sub>4</sub> expressed in terms of CO<sub>2</sub> equivalents (CO<sub>2</sub>e) during the study period totaled to -55 g CO<sub>2</sub>e m<sup>-2</sup> year<sup>-1</sup> (net CO<sub>2</sub>e sink) and 1147 g CO<sub>2</sub>e m<sup>-2</sup> year<sup>-1</sup> (net CO<sub>2</sub>e source) by using 100-year and 20-year global warming potential



values, respectively. Consequently, the ecosystem was almost CO<sub>2</sub>e neutral during the study period expressed on a 100-year time horizon but was a significant CO<sub>2</sub>e source on a 20-year time horizon.

## 35 1 Introduction

Wetland ecosystems play a disproportionately large role in the global carbon (C) cycle compared to the surface area they occupy. Wetlands cover only 6%–7% of the Earth's surface (Lehner and Döll, 2004), but they act as a major sink for the long-term storage of C by sequestering carbon dioxide (CO<sub>2</sub>) from the atmosphere. For example, strong C sinks (-621 and -597 g CO<sub>2</sub>-C m<sup>-2</sup> year<sup>-1</sup>) were found for temperate wetlands in Ontario, Canada and Siberia, respectively (den Hartog et al., 1994; Schulze et al., 1999). Other wetlands around the world sequester from -146 to -266 g CO<sub>2</sub>-C m<sup>-2</sup> year<sup>-1</sup> (Lafleur et al., 2001; Pihlatie et al., 2010; Shurpali et al., 1995). C storage in wetlands has been estimated to be up to 450 Gt C or approximately 20% of the total C storage in the terrestrial biosphere (Gorham, 1991; Maltby and Immirzi, 1993). However, wetlands emit significant quantities methane (CH<sub>4</sub>), a powerful GHG, due to anaerobic microbial decomposition (Aurela et al., 2001; Rinne et al., 2007). CH<sub>4</sub> emissions from wetlands are responsible for 30% of all global CH<sub>4</sub> emissions (Ciais et al., 2013). Peatlands are the most widespread of all wetland types in the world, representing 50 to 70% of global wetlands (Mundava, 2011). Their dynamics have played an important role in the global C cycle during the Holocene period (Gorham, 1991; Yu, 2011), and it has been shown that including peatlands in the modelling and analysis of the global C cycle to mitigate the changes in other C reservoirs is highly relevant (Brovkin et al., 2002; Kleinen et al., 2010; Menviel and Joos, 2012).

Many peatlands have been harvested and continue to be disturbed by the extraction of peat for horticultural use. In the case of Burns Bog, peat was also used for fire bombs during World War II (Cowen, 2015). Generally, during harvesting, the surface vegetation is removed, and then wetlands are drained by a network of ditches (Price and Waddington, 2000; Waddington and Roulet, 2000). When no longer economical, many harvested peatlands are abandoned and kept at artificially low water tables due to the drainage ditches. This environmental condition limits the disturbed and abandoned peatlands ability to return to their prior state. Drainage results in increased oxidation in peat soils, which then can become a strong source of CO<sub>2</sub> (Langeveld et al., 1997; Petrescu et al., 2015; Tapio-Biström et al., 2012). Additionally, degraded peat an increased fire risk, which can produce significant CO<sub>2</sub> emissions (Gaveau et al., 2014; Page et al., 2002; van der Werf et al., 2004). These consequences could be worse if nothing is done after the peat extraction. Therefore, and for reasons of conservation ecology (unique habitat), disturbed peatlands may be restored.

Restoration efforts typically rely on elevating the water table and managing vegetation. The water table depth and the amount of vegetation are the most important factors affecting land-atmosphere C exchange. Rewetting by ditch blocking can have an immediate impact on the C exchange between the peatland surface and the atmosphere (Limpens et al., 2008). Rewetting has strong direct and indirect effects on CO<sub>2</sub> and CH<sub>4</sub> fluxes. Raising the water level has been found to suppress the CO<sub>2</sub> efflux from the soil and result in an increase in net CO<sub>2</sub> uptake by native bog vegetation (Komulainen et al., 1999).



65 CH<sub>4</sub> emissions from rewetted sections in a bog in Finland were three times higher than the release from the disturbed and dry  
area (Tuittila et al., 2000). Another study found similar rates of CH<sub>4</sub> production in disturbed and restored wetlands in the  
southern United States (Schipper and Reddy, 1994). Re-vegetation of degraded peat leads to faster re-establishment of peat  
formation that can have significant effects on C exchange. However, the increased above- and below-ground biomass of  
70 plants and litter enhances organic matter oxidation, which raises CO<sub>2</sub> emissions (Finér and Laine, 1998; Minkkinen and  
Laine, 1998). In another study, re-establishing the conditions permitting peat formation also initially increased CH<sub>4</sub>  
emission, but the C exchange did not reach the level of seasonal emissions from pristine peatlands (Crill et al., 1992; Dise et  
al., 1993; Shannon and White, 1994).

Very few studies provide continuous, long-term measurements to determine how restored and rewetted peatland  
ecosystems recover in terms of their productivity and GHG exchange. It remains unclear when, or even if, restored peatland  
75 ecosystems could show a similar magnitude of C fluxes as in pristine (undisturbed) peatland ecosystems. Furthermore, most  
investigation focusing on GHG exchange of restored peatlands only measured CO<sub>2</sub> and/or CH<sub>4</sub> fluxes during short periods,  
e.g. the growing season. There are few studies that measured continuously and year-round fluxes (Anderson et al., 2016;  
Järveoja et al., 2016; Knox et al., 2015; Richards and Craft, 2015; Strack and Zuback, 2013), relying instead on sporadic, or  
repeating chamber measurements, which are difficult to upscale to annual totals.

80 In this study, we a) quantified seasonal and annual CO<sub>2</sub> and CH<sub>4</sub> fluxes, using the eddy covariance (EC) technique, in a  
disturbed ecosystem that is representative of areas subject to recent restoration efforts (ditch blocking for the last 8 years), b)  
identified key environmental controls and their effects on CO<sub>2</sub> and CH<sub>4</sub> fluxes, and c) quantified whether the study  
ecosystem is net source or sink of C and its net climate forcing at different time scales by considering GWPs of CO<sub>2</sub> and  
CH<sub>4</sub>.

## 85 2 Study area

Burns Bog in Delta, BC, on Canada's Pacific Coast, is part of a remnant peatland ecosystem that is recognized as the largest  
raised bog ecosystem on North America's west coast. During the last century, it was significantly disturbed as a result of it  
being used for housing, peat mining and agriculture (MetroVancouver, 2007). The Burns Bog Ecological Conservancy Area  
(BBECA) was established in 2005 to conserve this large coastal raised bog and restore ecological integrity to the greatest  
90 extent possible. Christen et al. (2016) measured summertime CO<sub>2</sub> and CH<sub>4</sub> exchanges using primarily chamber systems in  
several plots representative of disturbed areas of the BBECA, where some plots were rewetted and others were not. The  
study found substantial emissions of CH<sub>4</sub> primarily in recently rewetted plots, with highest emissions found under a high  
water table. Nevertheless, a significant spatial and temporal variability was found between and within plots. In order to  
constrain these emission estimates, it was suggested to extend the year-round monitoring of CO<sub>2</sub> and CH<sub>4</sub> exchanges using  
95 EC technique to provide spatially more representative fluxes at a recently rewetted plot.



The current study site is located in a harvested, disturbed, and rewetted area in the centre of the BBECA (122°59'05.87"W, 49°07'47.20"N, WGS-84) with dimensions of 400 m by 250 m. The field is surrounded by a windbreak to the west and an abandoned (now blocked) drainage ditch to the north (see supplementary material, Fig. S1 and S2). The study area was harvested between 1957 and 1963 using the Atkins-Durbrow Hydropeat method to remove the peat  
100 (Heathwaite and Göttlich, 1993). In 2007, the study site was rewetted via ditch-blocking using dams built with plywood and using wooden stakes as bracing (Howie et al., 2009). Following rewetting, water table height (WTH) in the study area fluctuates between 30 cm above ground and 20 cm below ground over the year. In all years since rewetting started in 2007, water table positions were lower in late summer and early fall and high all winter and spring. WTH decreases steadily  
105 between June and September. In September and October, the water table rises due to the increase in precipitation and the reduced evapotranspiration as a consequence of senescence. The depth of peat at the study site is 5.83 m. A silty clay layer is located below the peat layer (Chestnutt, 2015). The plant communities in the study ecosystem are dominated by *Sphagnum* spp. and *Rhynchospora alba*. The average height of the vegetation during the growing season is about 0.3 m (Madrone Consultants Ltd., 1999). Plants are separated by shallow open water pools, some of them populated by algae developing. Birch trees are dispersed and appear to be growing on the remnants of baulks but none of them was taller 2 m. Sphagnum  
110 covers over 25% of the surface inside the study area (Hebda et al., 2000). The area of the open water ponds was estimated to be about 20% of the surface in summer by aerial photo.

### 3 Materials and methods

#### 3.1 Climate measurements

Weather variables were continuously measured in order to determine climatic controls of CO<sub>2</sub> and CH<sub>4</sub> fluxes. Four  
115 components of radiation (shortwave/longwave, incoming and outgoing) were continuously measured by a four-component net radiometer (CNR1, Kipp and Zonen, Delft, Holland) on top of the tower. Two quantum sensors (LI-190, LI-COR Inc., Lincoln, NE, USA) measured incoming and outgoing photosynthetically active radiation (PAR). Precipitation was measured with an unheated tipping bucket rain gauge (TR-525M, Texas Electronics, Dallas, TX, USA) at 1 m height, 10 m north of the tower. Air temperature ( $T_a$ ) and relative humidity (RH, HMP-35 A, Vaisala, Finland) were measured at the heights of 2.0 m  
120 and 0.3 m, and soil thermocouples (type T) were recording soil/water temperatures at the depths of 0.05, 0.10 and 0.50 m. A pressure transducer (CS400, CSI) was installed on July 28<sup>th</sup> 2015 in an observation well west of the tower to continuously measure WTH for the remainder of the study period.

#### 3.2 Eddy-covariance measurements

Over the entire annual study period, from 16<sup>th</sup> June 2015 to 15<sup>th</sup> June 2016, a long-term eddy-covariance system (EC-1) was  
125 operated on a floating scaffold tower (Fig. 1) at a height of 1.8 m (facing south). The EC-1 system consisted of an ultrasonic anemometer-thermometer (CSAT-3, Campbell Scientific Inc. (CSI)) and an open-path CO<sub>2</sub>/H<sub>2</sub>O infrared gas analyzer



(IRGA, LI-7500, LI-COR Inc.). The path separation between CSAT-3 and LI-7500 was 5 cm. The CSAT-3 measured three-dimensional wind ( $u$ ,  $v$ ,  $w$ , in  $\text{m s}^{-1}$ ) and sonic temperature ( $T_s$ , in  $^{\circ}\text{C}$ ) at 60 Hz and output data at 10 Hz. The IRGA measured water vapor density ( $\rho_v$ ) and  $\text{CO}_2$  density ( $\rho_c$ ) at 10 Hz. The 10-Hz data from both instruments were sampled on a data  
 130 logger (CR1000, CSI) and processed fluxes of  $\text{CO}_2$  ( $F_c$ ) were calculated over 30 min blocks following the procedures documented in Crawford et al. (2013).

An additional, independent EC system (EC-2) was added on June 10<sup>th</sup> 2015 to measure  $\text{CH}_4$  fluxes. The EC-2 system was also located at a height of 1.8 m, 1.8 m to the west of EC-1, and faced south (Fig. 1). EC-2 consisted of a similar ultrasonic anemometer-thermometer (CSAT-3, CSI, 20 Hz), an enclosed-path  $\text{H}_2\text{O}/\text{CO}_2$  IRGA (LI-7200, LI-COR Inc. 20  
 135 Hz) and an open-path gas analyzer to measure the partial density of  $\text{CH}_4$  ( $\rho_m$ ) (LI-7700, LI-COR Inc., 20 Hz). The northward-separation of LI-7200 was 20 cm. The northward-separation of LI-7700 was 40 cm and eastward-separation of LI-7700 was 20 cm. Data from EC-2 were collected by an analyzer interface unit (LI-7550, LI-COR Inc.) and processed on-site. Fluxes of  $\text{CH}_4$  ( $F_m$ ) were processed in advanced mode using EddyPro® (V6.1.0, LI-COR Inc.) with a missing sample allowance of 30%.  $F_m$  data were quality checked using the flagging system proposed by Mauder and Foken (2004).

### 140 3.3 Gap filling algorithms

Some gaps in climate and flux measurements are unavoidable due to challenging weather and low-light situations (the station was solar powered), and need to be filled in for estimating seasonal and annual fluxes. Gaps in climate data (<1% of a year) were filled using measurements at nearby climate stations as documented in Lee et al. (2016). Small gaps (<60 minutes) of missing  $\text{CO}_2$  and  $\text{CH}_4$  fluxes were filled by linear interpolation. Longer gaps were filled using empirical  
 145 relationships between  $\text{CO}_2$  or  $\text{CH}_4$  fluxes and environmental variables. Two-year (from July 2014 to June 2016) of measurements of  $\text{CO}_2$  fluxes were used for modelling  $R_e$  and GEP to achieve better statistical relationships. Since there were two EC systems running with redundant fluxes of  $\text{CO}_2$ , the sensitivity of different combinations of data (EC-1 vs. EC-2 or using an average of the two) have been explored in Lee et al. (2016). For the data presented in this study,  $\text{CO}_2$  fluxes,  $H$ ,  $LE$  from EC-1 and  $\text{CH}_4$  fluxes EC-2 were used. Valid data from EC-1 was obtained for 59% of the year (after quality control).  
 150 Valid data from EC-2, which was restricted by power availability, was 32% of the year (after quality control).

#### 3.3.1 Gap filling of $\text{CO}_2$ flux data

For gaps longer than 2 hours in  $\text{CO}_2$  fluxes, the  $\text{CO}_2$  flux (e.g., net ecosystem exchange, NEE) was modelled as the difference between ecosystem respiration ( $R_e$ ) and gross ecosystem photosynthesis (GEP) i.e.  $\text{NEE} = R_e - \text{GEP}$ . Nocturnal NEE values were  $R_e$  as there is no photosynthesis (GEP) at night.

155  $R_e$  was modelled based on soil temperature at the 5-cm depth ( $T_{s,5cm}$ ) using a logistic fit (Neter et al., 1988):

$$R_e = \frac{1}{r_1 r_2 T_{s,5cm} + r_3} \quad (1)$$



160 A comparable logistic function was proposed and used by FLUXNET Canada (Barr et al., 2002; Kljun et al., 2006). In this study, we used this logistic model available in IDL (version 8.5.1, Exelis Visual Information Solutions, Boulder, Colorado).  $r_1$ ,  $r_2$ , and  $r_3$  are empirical parameters;  $r_1$  controls the slope of exponential phase;  $r_2$  decides where the transitional phase starts; and  $r_3$  determines the height of plateau phase. The empirical parameters  $r_1$ ,  $r_2$ , and  $r_3$  were determined separately for each day of the year, using a moving window of 120 days (60 days into past and 60 days into future) based on all measured nighttime data from 2014 to 2016 when friction velocity was higher than  $0.08 \text{ m s}^{-1}$ . Lee (2016) determined the effect of using different window sizes (60, 90, 120 and full year) on the annual modelled and gap-filled  $R_e$  and showed that a moving window size of 120 days was least sensitive to errors while still allowing for seasonal changes. However, sensitivity of choosing different window sizes on gap filled  $R_e$  was small, varying the annual value between 221 and  $229 \text{ g C m}^{-2} \text{ year}^{-1}$ .

165 GEP was modelled using the photosynthetic light-response curves (Ögren and Evans, 1993) based on photosynthetic photon flux density (PPFD in  $\mu\text{mol m}^{-2} \text{ s}^{-1}$ ):

170

$$\text{GEP} = \frac{MQY \cdot \text{PPFD} + P_M - ((MQY \cdot \text{PPFD} + P_M)^2 - 4 \cdot C_v \cdot MQY \cdot \text{PPFD} \cdot P_M)^{0.5}}{2 \cdot C_v} \quad (2)$$

Maximum photosynthetic rate at light saturation ( $P_M$ ) and maximum quantum yield ( $MQY$ ) are fitted parameters with GEP estimated as measured daytime NEE minus daytime  $R_e$  calculated using Eq. 1. Convexity ( $C_v$ ) was fixed at 0.7 (Farquhar et al., 1980). The time-varying parameters  $MQY$  and  $P_M$  were fitted separately for each day, using a moving window of 90 days using all data from 2014 to 2016 when friction velocity was higher than  $0.08 \text{ m s}^{-1}$ . The sensitivity of window size on gap filled GEP was small, resulting in annual value to vary between 385 and  $415 \text{ g C m}^{-2} \text{ year}^{-1}$ .

### 3.3.2 Gap filling of $\text{CH}_4$ flux data

180  $\text{CH}_4$  fluxes with quality flags 0 and 1 according to Mauder and Foken (2004) were plotted against all related variables including WTH,  $\theta_w$ ,  $T_a$ , and  $T_{s,5cm}$ . Since the main control was  $T_{s,5cm}$ , it was used to build a model to fill the gaps in  $\text{CH}_4$  fluxes:

$$F_m = a e^{b T_{s,5cm}} \quad (3)$$

185 where  $F_m$  is the  $\text{CH}_4$  flux,  $T_{s,5cm}$  is the soil temperature at the 5 cm depth, and  $a$  and  $b$  are empirical parameters for the annual relationship.



### 3.4 Calculating CO<sub>2</sub>e

The combined effect all long-lived greenhouse gases was compared for CO<sub>2</sub> and CH<sub>4</sub> by converting the molar fluxes of CO<sub>2</sub> and CH<sub>4</sub> into time-integrated radiative forcing (e.g. global warming potential, GWP) expressed on a mass basis in terms of CO<sub>2</sub> equivalents (g CO<sub>2</sub>e m<sup>-2</sup> s<sup>-1</sup>) as follows:

$$CO_2e \text{ (g)} = m_{CO_2}F_{CO_2} + GWP_{CH_4}m_{CH_4}F_{CH_4} \quad (4)$$

$GWP_{CH_4}$  is the mass-based GWP for the CH<sub>4</sub> (g g<sup>-1</sup>),  $m_{CO_2}$  is the molecular mass of CO<sub>2</sub> (g mol<sup>-1</sup>), and  $m_{CH_4}$  is the molecular mass of CH<sub>4</sub> (g mol<sup>-1</sup>). In this study, a 100-year GWP of CH<sub>4</sub> of 28, and 20-year GWP of CH<sub>4</sub> of 84, were used respectively (IPCC, 2014). N<sub>2</sub>O fluxes have been neglected in this study because previous chamber-based measurements during the growing season found no significant emissions or uptake of N<sub>2</sub>O in all study plots in the BBCEA (Christen et al., 2016).

## 4 Results and Discussion

### 4.1 Weather

During the study period (June 16<sup>th</sup> 2015 to June 15<sup>th</sup> 2016), the site experienced an annual average  $T_a$  (2 m height) of 11.3 °C. Mean monthly  $T_a$  ranged between 4.4 (Jan 2016) and 19.3 °C (Jul 2015). The study site received a total annual precipitation of 1061.7 mm, of which 16% (173.4 mm) fell during the warm half year (Apr-Sep) and 84% (888.3 mm) during the cold half year (Oct-Mar). There was no lasting snow cover during the study year. However, the surface was frozen over ten days in January 2016, with an ice thickness of up to 5 cm.

Winds at this site were often influenced by a sea-land breeze circulation. Under sea-breeze situations, wind mainly came from the south (40% of all cases). Sometimes, however, the sea-land breeze blew from the west, primarily between 17:00 and 19:00 PST. The wind direction on average turned to east during the nighttime (land-breeze), and generally at night, the winds were weaker.

### 4.2 Surface conditions

#### 4.2.1 Turbulent flux footprints

Cumulative turbulent source areas were calculated using the analytical turbulent source area (turbulent footprint) model from Kormann and Meixner (Kormann and Meixner, 2001) following the procedure outlined in Christen et al. (2011). The 80% contour line (enclosing 80% of the cumulative probability for a unit source) was entirely inside the field in spring and summer. It reached beyond the ditches at the north side in fall and winter. Unstable conditions during daytime allowed for a more constrained footprint surrounding the tower. Stable conditions at night led to larger footprints, primarily from East. The



cumulative footprint for each of the four seasons for the EC-1 overlaid on the satellite image of the site are documented in Fig. S1 (supplementary material).

#### 4.2.2 Vegetation cover and water table changes

220 Mosses and sedges started to grow in March and grasses grew up to a maximum of 0.3 m height in summer. In summer, vegetation covered almost the entire study area of the surface, including ponds (some with algae), so the surface was less patchy in summer compared to other seasons, when standing water ponds were intermixed with vegetation in fall, winter and spring (see supplementary material, Fig. S2).

225 Winter was the wettest season when WTH was mostly above the bare soil (reference surface). The highest water table position was 7.7 cm above the reference surface in December. In the dry season, the water table position dropped to 26.5 cm beneath the bog surface in August. The WTH decreased in spring, and dry hummocks could be seen from April to September. The water table started to rise above the surface after receiving the fall precipitation. The study site was flooded in winter during the study year.

#### 4.3 CO<sub>2</sub> exchange

##### 4.3.1 Annual, seasonal and monthly NEE, $R_e$ and GEP

230 Overall, the study area was a CO<sub>2</sub> sink in spring (MAM,  $-1.10 \text{ g C m}^{-2} \text{ day}^{-1}$ ) and in summer (JJA,  $-0.82 \text{ g C m}^{-2} \text{ day}^{-1}$ ). Net CO<sub>2</sub> fluxes were near zero in fall (SON,  $+0.03 \text{ g C m}^{-2} \text{ day}^{-1}$ ) and winter (DJF,  $-0.07 \text{ g C m}^{-2} \text{ day}^{-1}$ ). Over the entire year, the annual CO<sub>2</sub>-C budget (i.e., NEE) was  $-179 \text{ g C m}^{-2} \text{ yr}^{-1}$ . Almost in each month of the calendar year, the site was a weak sink for CO<sub>2</sub> except in October, November and December (Fig. 2, Table 1). Monthly net fluxes of CO<sub>2</sub> (NEE) ranged from  $+1.77 \text{ g C m}^{-2} \text{ month}^{-1}$  in November 2015 to  $-56.20 \text{ g C m}^{-2} \text{ month}^{-1}$  in May 2016.

235 The annual  $R_e$  and GEP during the study year were 236 and  $415 \text{ g C m}^{-2} \text{ yr}^{-1}$ , respectively. The relative changes in  $R_e$  and GEP were closely linked to the seasonality of the plant phenology. Based on GEP trends, we can divide the study period into three segments, ‘winter’ (Oct-Mar), ‘early growing season’ (Apr-Jun), and ‘late growing season’ (Jul-Sep). The rising temperature triggered growth in the early growing season (GEP =  $59.73 \text{ g C m}^{-2} \text{ month}^{-1}$ ), while the later growing season had limited growth (GEP =  $25.08 \text{ g C m}^{-2} \text{ month}^{-1}$ ). Winter had lowest productivity (GEP =  $7.58 \text{ g C m}^{-2} \text{ month}^{-1}$ ) (Table 1).  
240 Despite a large seasonal amplitude in monthly GEP,  $R_e$  showed less variability over the year. The highest increasing rate of NEE and the highest magnitude of NEE both occurred in May during the early growing season (Fig. 2). This was caused by the onset of  $R_e$  being delayed compared to GEP, resulting in the greatest imbalance between respiratory and assimilatory fluxes in May.

245 Table 2 compares annual NEE,  $R_e$  and GEP at the study site to Fluxnet sites over other land covers in the same region that experienced similar climate forcings, although from different years. An unmanaged grassland site 15 km to the west of the study area in the Fraser River Delta (Westham Island, Delta, BC, Crawford et al., 2013) had about 1.3 times higher NEE





than this rewetted area. Annual  $R_e$  and GEP values at this grassland site were higher than the study site by a factor of 5.2 and 3.5. A mature 55-year-old Douglas-fir forest on Vancouver Island (200 km NW of the study area; Krishnan et al., 2009) showed an NEE of 1.8 times higher than the study area. The  $R_e$  and GEP were even higher by factors of 7.8 and 5.2, respectively. A young forest plantation (Buckley Bay, 150 km W of the study area; Krishnan et al., 2009), which was a weak C source, had  $R_e$  and GEP of six- and three-fold higher than the study site, respectively. Compared to these other sites under similar climatic conditions, the rewetted area of the bog was not an ecosystem of high productivity but one with considerably limited  $R_e$  that permits more efficient  $\text{CO}_2$  sequestration (-NEE is 43 % of GEP, as opposed to 15% for the unmanaged grassland site and mature forest).

#### 255 4.3.2 Diurnal variability in $\text{CO}_2$ fluxes

The seasonally-changing diurnal course of gap-filled NEE with isopleths over time of day and year is shown in Fig. 3. The daily maximum GEP changed seasonally, consequently the highest NEE was observed during midday between May and July ( $-3.5 \mu\text{mol m}^{-2} \text{s}^{-1}$ ). During nighttime,  $R_e$  was less varying with season, and on average was  $\leq 1 \mu\text{mol m}^{-2} \text{s}^{-1}$  for most of the study period.

#### 260 4.3.3 Ecosystem respiration

Figure 4 shows the relationship between nighttime  $R_e$  and  $T_{s,5cm}$  using the data for the entire study period.  $R_e$  increased with increasing  $T_{s,5cm}$  as expected, and annually followed a logistic curve rather than an exponential relationship.  $R_e$  response curves were also calculated every two months (see supplementary material, Fig. S3).  $R_e$  showed different curves depending on season. In winter,  $R_e$  varied little with  $T_{s,5cm}$  and was close to zero. From February to May, the relationship became closer to logistic. In June and July, the fitted curve stayed at  $1 \mu\text{mol m}^{-2} \text{s}^{-1}$  because  $T_{s,5cm}$  remained above  $15^\circ\text{C}$ . The study area had the highest  $R_e$  in these two months. In fall,  $R_e$  curves were closer to an exponential relationship, which could be due in part to leaf senescence (Shurpali et al., 2008). Decomposition of dead plant organic matter on the soil surface may have caused a higher  $R_e$  in fall compared to spring and winter at the same  $T_{s,5cm}$ . Another factor could be the WTH, which in fall was not high enough to suppress  $R_e$  as it did in winter (Juszczak et al., 2013). The differences between March and September at the same  $T_{s,5cm}$  were up to  $0.4 \mu\text{mol m}^{-2} \text{s}^{-1}$ .

Two other controls on  $R_e$  explored were air temperature ( $T_a$ ) and WTH.  $T_a$  did have a similar impact on  $R_e$  as  $T_{s,5cm}$  when  $T_a < 16^\circ\text{C}$ , but for warmer temperatures,  $T_a$  did not correlate with  $R_e$ . The explanation for this is that heterotrophic component of  $R_e$  depends on  $T_s$ , not the rapidly changing  $T_a$  (Davidson et al., 2002; Edwards, 1975; Lloyd and Taylor, 1994).

It is widely reported that in most terrestrial ecosystems, the activity of soil microbes is also governed by soil moisture status, having little activity when the soil is excessively dry or excessively wet. Accordingly, and like other wetlands,  $R_e$  was small when the water table was above the surface because this situation suppressed aerobic decomposition of peat (Rochefort et al., 2002; Weltzin et al., 2000). When the water table was below surface,  $R_e$  increased to near  $1 \mu\text{mol m}^{-2} \text{s}^{-1}$  and became stable no matter how low the water table position was. This relationship was also found in many other peatlands (Bridgman



et al., 2006; Ellis et al., 2009; Strack et al., 2006). There was no obvious relationship between  $\theta_w$  (integrated from 0-30 cm  
 280 depth) and  $R_e$ .  $R_e$  slightly decreased from 1.0 to 0.6  $\mu\text{mol m}^{-2} \text{s}^{-1}$  when  $\theta_w$  increased from 84% to 88%. Other than this range,  
 $\theta_w$  had no more impact on  $R_e$ .

#### 4.3.4 Gross ecosystem photosynthesis

Figure 5 shows the average light response curve, with half-hourly GEP as a function of PPFD. Due to different phenology  
 over the year and the changes in solar altitude, light response curves were also calculated every two months (see  
 285 supplementary material, Fig. S4). GEP reached a maximum in May with 92.63 g C  $\text{m}^{-2} \text{month}^{-1}$ , and a minimum of 2.79 g C  
 $\text{m}^{-2} \text{month}^{-1}$  in December (Fig. 2, Table 1). GEP at light saturation reached roughly 5.09  $\mu\text{mol m}^{-2} \text{s}^{-1}$  in summer, and  
 remained below 2.49  $\mu\text{mol m}^{-2} \text{s}^{-1}$  in winter, due to reduced leaf area, flooding, and lower temperatures. From March to May,  
 GEP increased much more rapidly than  $R_e$ . In fall, GEP decreased faster than  $R_e$ . The magnitude of  $R_e$  already was close to  
 GEP in the late August to make the study area become CO<sub>2</sub> neutral in late summer.

290 Other possible controls on GEP explored were  $T_a$  and WTH. To exclude the primary driver, PAR, here only data when  
 PAR was between 300 and 500  $\mu\text{mol m}^{-2} \text{s}^{-1}$  (light had no effect on GEP) were used. We found out there was the light-  
 independent photosynthesis which occurs in the stoma depending on  $T_a$  (Calvin, 1962) in the study area. Between 0 and 10  
 $^{\circ}\text{C}$   $T_a$ , photosynthesis was low even when supplied by ample PAR due to low leaf area during that period. A rapid increase in  
 GEP was found from 10 to 15  $^{\circ}\text{C}$ . When  $T_a$  was higher than 15  $^{\circ}\text{C}$ , WTH did not show any direct influence on GEP.

### 295 4.4 CH<sub>4</sub> exchange

#### 4.4.1 Annual and seasonal CH<sub>4</sub> budgets

Overall, the study area was a source of CH<sub>4</sub> in each of the twelve months (Table 1). The annual CH<sub>4</sub>-C budget was 16 g CH<sub>4</sub>-  
 C  $\text{m}^{-2} \text{yr}^{-1}$ . CH<sub>4</sub> emissions were close to zero in winter (8.7 mg CH<sub>4</sub>-C  $\text{m}^{-2} \text{day}^{-1}$ ). It was a weak CH<sub>4</sub> source in fall (21.5 mg  
 CH<sub>4</sub>-C  $\text{m}^{-2} \text{day}^{-1}$ ) and spring (29.4 mg CH<sub>4</sub>-C  $\text{m}^{-2} \text{day}^{-1}$ ), and then became a significant source in summer (120.9 mg CH<sub>4</sub>-C  
 300  $\text{m}^{-2} \text{day}^{-1}$ ). Monthly emissions of CH<sub>4</sub> ranged from 66 (November) to 4436 (July) mg CH<sub>4</sub>-C  $\text{m}^{-2} \text{month}^{-1}$ . CH<sub>4</sub> fluxes showed  
 a seasonal pattern, which was linked to phenology and temperature. The rising  $T_a$  did not trigger CH<sub>4</sub> production  
 immediately, and CH<sub>4</sub> fluxes remained low in April and May. But once the subsurface and water became warm enough, CH<sub>4</sub>  
 emissions increased from 1.5 to 3.0 g CH<sub>4</sub>-C  $\text{m}^{-2} \text{month}^{-1}$  in June (Table 1). CH<sub>4</sub> emissions reached the peak in July (4.4 g  
 CH<sub>4</sub>-C  $\text{m}^{-2} \text{month}^{-1}$ ) and held similar magnitude (3.7 g CH<sub>4</sub>-C  $\text{m}^{-2} \text{month}^{-1}$ ) in August even though the  $T_a$  had dropped.

#### 305 4.4.2 Diurnal variability in CH<sub>4</sub> fluxes

The ensemble diurnal courses of the gap-filled CH<sub>4</sub> fluxes (measured CH<sub>4</sub> emissions and gap-filled by modelled CH<sub>4</sub> fluxes)  
 by the EC-2 system are shown in Fig. 6 from June 16<sup>th</sup> 2015 to June 15<sup>th</sup> 2016. Surprisingly, there was not much of a diurnal  
 course observed for CH<sub>4</sub> fluxes. CH<sub>4</sub> was continuously emitted through day and night. Thermal effects such as recently



reported by Poindexter et al., 2016 were not found. From January to March and October to December, the study site had  
310 constant CH<sub>4</sub> emissions of less than 50 nmol m<sup>-2</sup> s<sup>-1</sup>, and almost no diurnal variation was observed. July had the greatest CH<sub>4</sub>  
emissions, and the highest magnitude (>150 nmol m<sup>-2</sup> s<sup>-1</sup>) appeared in the evening (3 pm to 9 pm). This corresponded to the  
lagged effect to soil temperature.

#### 4.5 CO<sub>2</sub>e exchange

Figure 7a and 7b show CO<sub>2</sub> and CH<sub>4</sub> fluxes expressed in terms of CO<sub>2</sub>e using 100-year and 20-year GWPs, respectively.  
315 Considering fluxes of both GHGs together, this rewetted area was annually near to CO<sub>2</sub>e neutral at 100-year scale with a net  
uptake by CO<sub>2</sub> (-656 g CO<sub>2</sub>e m<sup>-2</sup> year<sup>-1</sup>) nearly the same as CH<sub>4</sub> emissions (601 g CO<sub>2</sub>e m<sup>-2</sup> year<sup>-1</sup>). On shorter time horizon  
of 20 years, the study area represented a significant net climatic forcing in CO<sub>2</sub>e terms as the net uptake of CO<sub>2</sub> (-656 g CO<sub>2</sub>e  
m<sup>-2</sup> year<sup>-1</sup>) was one-third that of CH<sub>4</sub> emissions (1803 g CO<sub>2</sub>e m<sup>-2</sup> year<sup>-1</sup>). In late spring and early summer, the early onset of  
CO<sub>2</sub> sequestration in May and the time lag in CH<sub>4</sub> fluxes combined to represent a negative net GHG forcing, no matter  
320 which GWP time horizon was considered. The quick drop in CO<sub>2</sub> sequestration in August and September allowed the  
highest net GHG forcing to be observed at both time horizons in late summer. In short, the critical time period for both, CO<sub>2</sub>  
and CH<sub>4</sub> fluxes, was the growing season when magnitude of fluxes changed differently across the growing season. The  
results show that measurements made during a part of the growing season are not necessarily representative for the entire  
growing season or the year. Christen et al., 2016 found that CH<sub>4</sub> emissions exceeded CO<sub>2</sub> uptake by a factor of 50 using  
325 GWPs at 100-year time horizon in July and August in a recently rewetted areas of the BBECA. During spring and early  
summer (April and May), however, CO<sub>2</sub> uptake can exceed CH<sub>4</sub> emissions.

#### 5 Conclusions

The study area, a rewetted plot in the BBECA undergoing ecological restoration, was a net CO<sub>2</sub> sink over the study period (-  
179 g CO<sub>2</sub>-C m<sup>-2</sup> year<sup>-1</sup>). The study area was not a highly productive ecosystem (annual GEP = 415 g CO<sub>2</sub>-C m<sup>-2</sup> year<sup>-1</sup>) but  
330 exhibited low *R<sub>e</sub>* (annual *R<sub>e</sub>* = 236 g CO<sub>2</sub>-C m<sup>-2</sup> year<sup>-1</sup>), likely due to oxygen limitations. The annual CO<sub>2</sub> fluxes reported here  
from a restored and rewetted peatland are comparable with data reported from pristine temperate peatlands in temperate mid  
latitudes (Alm et al., 1997; Lafleur et al., 2001; Pihlatie et al., 2010; Shurpali et al., 1995). The study area sequestered less  
CO<sub>2</sub> than the few other restored wetlands reported in the literature (Anderson et al., 2016; Järveoja et al., 2016; Knox et al.,  
2015; Richards and Craft, 2015; Strack and Zuback, 2013). The major controls on CO<sub>2</sub> fluxes were PAR irradiance and  
335 *T<sub>s,5cm</sub>*. The magnitude of PAR strongly controlled GEP, and the *T<sub>s,5cm</sub>* regulated *R<sub>e</sub>*. WTH also had influence on *R<sub>e</sub>* especially  
when the ecosystem was flooded.

Annual CH<sub>4</sub> emissions were 16 g CH<sub>4</sub>-C m<sup>-2</sup> year<sup>-1</sup>, which is lower than those reported for other restored wetlands  
(Anderson et al., 2016; Knox et al., 2015). CH<sub>4</sub> emissions in summer months were 60 times stronger than in winter. The  
ditch blocking permitted anaerobic conditions with the water table within 30 cm of the surface throughout the year. Effects



340 of changing WTH on CH<sub>4</sub> fluxes at the study area were not clearly apparent.  $T_{s,5cm}$  explained CH<sub>4</sub> fluxes best ( $R^2 = 0.66$ ) –  
although both  $T_{s,5cm}$  and WTH changed seasonally.

In terms of the C balance, our results suggest that our study area in BBECA was a net C sink ( $-163 \text{ g C m}^{-2} \text{ year}^{-1}$ ) during  
the 8<sup>th</sup> year following rewetting. These results are consistent with those of several disturbed peatlands that have become a net  
annual C sink after following restoration by rewetting (Karki et al., 2016; Schrier-Uijl et al., 2014; Wilson et al., 2013). In  
345 terms of net climate forcing of the system related to CO<sub>2</sub> and CH<sub>4</sub> fluxes expressed by GWPs, our results show that the  
ecosystem was almost CO<sub>2</sub>e neutral ( $-55 \text{ g CO}_2\text{e m}^{-2} \text{ year}^{-1}$ ) over a 100-year time horizon during the study period after a  
7-year restoration. However, the rewetted area was a substantial net CO<sub>2</sub>e source ( $1147 \text{ g CO}_2\text{e m}^{-2} \text{ year}^{-1}$ ) on a 20-year  
time horizon due to the stronger GWP of CH<sub>4</sub> on shorter timescales.

### 350 Acknowledgements

This research was primarily funded through research contracts between Metro Vancouver and UBC (PI: Christen). Selected  
equipment was supported by the Canada Foundation for Innovation (Christen, Johnson) and NSERC RTI (Christen).  
Financial support through scholarships and training were provided by UBC Faculty of Graduate and Postdoctoral Studies  
and UBC Geography. We appreciate the substantial technical and logistical support by Joe Soluri (Metro Vancouver) in  
355 operating the site, and scientific contributions and data provided by C. Reynolds (Metro Vancouver) and S. Howie (Delta,  
BC).

### References

- Alm, J., Talanov, A., Saarnio, S., Silvola, J., Ikkonen, E., Aaltonen, H., Nykänen, H., and Martikainen, P. J.: Reconstruction  
of the carbon balance for microsites in a boreal oligotrophic pine fen, Finland, *Oecologia*, 110, 423-431, 1997.
- 360 Anderson, F. E., Bergamaschi, B., Sturtevant, C., Knox, S., Hastings, L., Windham-Myers, L., Detto, M., Hestir, E. L.,  
Drexler, J., Miller, R. L., Matthes, J. H., Verfaillie, J., Baldocchi, D., Snyder, R. L., and Fujii, R.: Variation of energy and  
carbon fluxes from a restored temperate freshwater wetland and implications for carbon market verification protocols,  
*Journal of Geophysical Research: Biogeosciences*, 121, 777-795, 2016.
- Aurela, M., Laurila, T., and Tuovinen, J.-P.: Seasonal CO<sub>2</sub> balances of a subarctic mire, *Journal of Geophysical Research:*  
365 *Atmospheres*, 106, 1623-1637, 2001.
- Barr, A. G., Griffis, T. J., Black, T. A., Lee, X., Staebler, R. M., Fuentes, J. D., Chen, Z., and Morgenstern, K.: Comparing  
the carbon budgets of boreal and temperate deciduous forest stands, *Canadian Journal of Forest Research*, 32, 813-822, 2002.
- Bridgham, S., Megonigal, J. P., Keller, J., Bliss, N., and Trettin, C.: The carbon balance of North American wetlands,  
*Wetlands*, 26, 889-916, 2006.



- 370 Brovkin, V., Bendtsen, J., Claussen, M., Ganopolski, A., Kubatzki, C., Petoukhov, V., and Andreev, A.: Carbon cycle, vegetation, and climate dynamics in the Holocene: Experiments with the CLIMBER-2 model, *Global Biogeochemical Cycles*, 16, 1139, 2002.
- Calvin, M.: The Path of Carbon in Photosynthesis, *Angewandte Chemie International Edition in English*, 1, 65-75, 1962.
- Chestnutt, C.: For peak's sake: A water balance study and comparison of the eddy covariance technique and semi-empirical calculation to determine summer evapotranspiration in Burns Bog, British Columbia., BSc, The University of Edinburgh, The University of British Columbia, 2015.
- 375 Christen, A., Coops, N. C., Crawford, B. R., Kellett, R., Liss, K. N., Olchovski, I., Tooke, T. R., van der Laan, M., and Voogt, J. A.: Validation of modeled carbon-dioxide emissions from an urban neighborhood with direct eddy-covariance measurements, *Atmospheric Environment*, 45, 6057-6069, 2011.
- 380 Christen, A., Jassal, R. S., Black, T. A., Grant, N. J., Hawthorne, I., Johnson, M. S., Lee, S. C., and M., M.: Summertime greenhouse gas fluxes from an urban bog undergoing restoration through rewetting., *Mires and Peat*, 18, 1-24, 2016.
- Ciais, P., Sabine, C., Bala, G., Bopp, L., Brovkin, V., Canadell, J., Chhabra, A., DeFries, R., Galloway, J., Heimann, M., Jones, C., Le Quéré, C., Myneni, R. B., Piao, S., and Thornton, P.: Carbon and Other Biogeochemical Cycles. In: *Climate Change 2013: The Physical Science Basis. Contribution of Working Group I to the Fifth Assessment Report of the Intergovernmental Panel on Climate Change*, Stocker, T. F., Qin, D., Plattner, G.-K., Tignor, M., Allen, S. K., Boschung, J., Nauels, A., Xia, Y., Bex, V., and Midgley, P. M. (Eds.), Cambridge University Press, Cambridge, United Kingdom and New York, NY, USA, 2013.
- 385 Cowen, G. J.: Social and environmental interaction in urban wetlands, Burns Bog Conservation Society., 2015.
- Crawford, B., Christen, A., and Ketler, R.: Processing and quality control procedures of turbulent flux measurements during the Vancouver EPiCC experiment, The University of British Columbia, 2013.
- 390 Crill, P., Bartlett, K., and Roulet, N.: Methane flux from boreal peatlands, International workshop on carbon cycling in boreal peatlands and climatic change, *Hyytiälae*, Finland, 10, 1992.
- Davidson, E. A., Savage, K., Verchot, L. V., and Navarro, R.: Minimizing artifacts and biases in chamber-based measurements of soil respiration, *Agricultural and Forest Meteorology*, 113, 21-37, 2002.
- 395 den Hartog, G., Neumann, H. H., King, K. M., and Chipanshi, A. C.: Energy budget measurements using eddy correlation and Bowen ratio techniques at the Kinosheo Lake tower site during the Northern Wetlands Study, *Journal of Geophysical Research: Atmospheres*, 99, 1539-1549, 1994.
- Dise, N. B., Gorham, E., and Verry, E. S.: Environmental factors controlling methane emissions from peatlands in northern Minnesota, *Journal of Geophysical Research: Atmospheres*, 98, 10583-10594, 1993.
- 400 Edwards, N. T.: Effects of Temperature and Moisture on Carbon Dioxide Evolution in a Mixed Deciduous Forest Floor1, *Soil Science Society of America Journal*, 39, 361-365, 1975.



- Ellis, T., Hill, P. W., Fenner, N., Williams, G. G., Godbold, D., and Freeman, C.: The interactive effects of elevated carbon dioxide and water table draw-down on carbon cycling in a Welsh ombrotrophic bog, *Ecological Engineering*, 35, 978-986, 2009.
- 405 Farquhar, G. D., von Caemmerer, S., and Berry, J. A.: A biochemical model of photosynthetic CO<sub>2</sub> assimilation in leaves of C<sub>3</sub> species, *Planta*, 149, 78-90, 1980.
- Finér, L. and Laine, J.: Root dynamics at drained peatland sites of different fertility in southern Finland, *Plant and Soil*, 201, 27-36, 1998.
- Foken, T., Gockede, M., Mauder, M., Mahrt, L., Amiro, B. D., and Munger, J. W.: Post-field data quality control. In:
- 410 *Handbook of Micrometeorology: A Guide for Surface Flux Measurements*, Lee, X. (Ed.), Kluwer Academic Publishers, Dordrecht, 2004.
- Gaveau, D. L. A., Salim, M. A., Hergoualc'h, K., Locatelli, B., Sloan, S., Wooster, M., Marlier, M. E., Molidena, E., Yaen, H., DeFries, R., Verchot, L., Murdiyarso, D., Nasi, R., Holmgren, P., and Sheil, D.: Major atmospheric emissions from peat fires in Southeast Asia during non-drought years: evidence from the 2013 Sumatran fires, *Scientific Reports*, 4, 6112, 2014.
- 415 Gorham, E.: Northern Peatlands: Role in the Carbon Cycle and Probable Responses to Climatic Warming, *Ecological Applications*, 1, 182-195, 1991.
- Heathwaite, A. L. and Göttlich, K.: *Mires: process, exploitation, and conservation*, Wiley, 1993.
- Hebda, R. J., Gustavson, K., Golinski, K., and Calder, A. M.: Burns Bog Ecosystem Review Synthesis for Burns Bog, Fraser River Delta, South-western British Columbia, Canada, Environmental Assessment Office, Victoria, B.C., 2000.
- 420 Howie, S. A., Whitfield, P. H., Hebda, R. J., Munson, T. G., Dakin, R. A., and Jeglum, J. K.: Water Table and Vegetation Response to Ditch Blocking: Restoration of a Raised Bog in Southwestern British Columbia, *Canadian Water Resources Journal / Revue canadienne des ressources hydriques*, 34, 381-392, 2009.
- IPCC: *Climate Change 2014: Impacts, Adaptation, and Vulnerability. Part A: Global and Sectoral Aspects. Contribution of Working Group II to the Fifth Assessment Report of the Intergovernmental Panel on Climate Change* [Field, C.B., V.R. Barros, D.J. Dokken, K.J. Mach, M.D. Mastrandrea, T.E. Bilir, M. Chatterjee, K.L. Ebi, Y.O. Estrada, R.C. Genova, B. Girma, E.S. Kissel, A.N. Levy, S. MacCracken, P.R. Mastrandrea, and L.L. White (eds.)], Cambridge University Press, Cambridge, United Kingdom and New York, NY, USA, 2014.
- 425 Järveoja, J., Peichl, M., Maddison, M., Soosaar, K., Vellak, K., Karofeld, E., Teemusk, A., and Mander, Ü.: Impact of water table level on annual carbon and greenhouse gas balances of a restored peat extraction area, *Biogeosciences*, 13, 2637-2651,
- 430 2016.
- Juszczak, R., Humphreys, E., Acosta, M., Michalak-Galczevska, M., Kayzer, D., and Olejnik, J.: Ecosystem respiration in a heterogeneous temperate peatland and its sensitivity to peat temperature and water table depth, *Plant and Soil*, 366, 505-520, 2013.
- Karki, S., Elsgaard, L., Kandel, T. P., and Lærke, P. E.: Carbon balance of rewetted and drained peat soils used for biomass
- 435 production: a mesocosm study, *GCB Bioenergy*, 8, 969-980, 2016.



- Kleinen, T., Brovkin, V., von Bloh, W., Archer, D., and Munhoven, G.: Holocene carbon cycle dynamics, *Geophysical Research Letters*, 37, L02705, 2010.
- Kljun, N., Black, T. A., Griffis, T. J., Barr, A. G., Gaumont-Guay, D., Morgenstern, K., McCaughey, J. H., and Nesic, Z.: Response of Net Ecosystem Productivity of Three Boreal Forest Stands to Drought, *Ecosystems*, 9, 1128-1144, 2006.
- 440 Knox, S. H., Sturtevant, C., Matthes, J. H., Koteen, L., Verfaillie, J., and Baldocchi, D.: Agricultural peatland restoration: effects of land-use change on greenhouse gas (CO<sub>2</sub> and CH<sub>4</sub>) fluxes in the Sacramento-San Joaquin Delta, *Global Change Biology*, 21, 750-765, 2015.
- Komulainen, V.-M., Tuittila, E.-S., Vasander, H., and Laine, J.: Restoration of Drained Peatlands in Southern Finland: Initial Effects on Vegetation Change and CO<sub>2</sub> Balance, *Journal of Applied Ecology*, 36, 634-648, 1999.
- 445 Kormann, R. and Meixner, F. X.: An analytical footprint model for non-neutral stratification, *Boundary-Layer Meteorology*, 99, 207-224, 2001.
- Krishnan, P., Black, T. A., Jassal, R. S., Chen, B., and Nesic, Z.: Interannual variability of the carbon balance of three different-aged Douglas-fir stands in the Pacific Northwest, *Journal of Geophysical Research: Biogeosciences*, 114, n/a-n/a, 2009.
- 450 Lafleur, P. M., Roulet, N. T., and Admiral, S. W.: Annual cycle of CO<sub>2</sub> exchange at a bog peatland, *Journal of Geophysical Research: Atmospheres*, 106, 3071-3081, 2001.
- Langeveld, C. A., Segers, R., Dirks, B. O. M., van den Pol-van Dasselaar, A., Velthof, G. L., and Hensen, A.: Emissions of CO<sub>2</sub>, CH<sub>4</sub> and N<sub>2</sub>O from pasture on drained peat soils in the Netherlands. In: *Developments in Crop Science*, Ittersum, M. K. v. and Geijn, S. C. v. d. (Eds.), Elsevier, 1997.
- 455 Lee, S.-C.: Annual greenhouse gas budget for a bog ecosystem undergoing restoration by rewetting, MSc, Geography, UBC, Vancouver, 2016.
- Lehner, B. and Döll, P.: Development and validation of a global database of lakes, reservoirs and wetlands, *Journal of Hydrology*, 296, 1-22, 2004.
- Limpens, J., Berendse, F., Blodau, C., Canadell, J. G., Freeman, C., Holden, J., Roulet, N., Rydin, H., and Schaepman-Strub, G.: Peatlands and the carbon cycle: from local processes to global implications – a synthesis, *Biogeosciences*, 5, 1475-1491, 2008.
- Lloyd, J. and Taylor, J. A.: On the Temperature Dependence of Soil Respiration, *Functional Ecology*, 8, 315-323, 1994.
- Madrone Consultants Ltd.: *Burns Bog Ecosystem Review. Plants and Plant Communities*. 1999.
- Maltby, E. and Immirzi, P.: Carbon dynamics in peatlands and other wetland soils regional and global perspectives, *Chemosphere*, 27, 999-1023, 1993.
- 465 Menviel, L. and Joos, F.: Toward explaining the Holocene carbon dioxide and carbon isotope records: Results from transient ocean carbon cycle-climate simulations, *Paleoceanography*, 27, PA1207, 2012.
- MetroVancouver: *Burns Bog Ecological Conservancy Area Management Plan*. 2007.

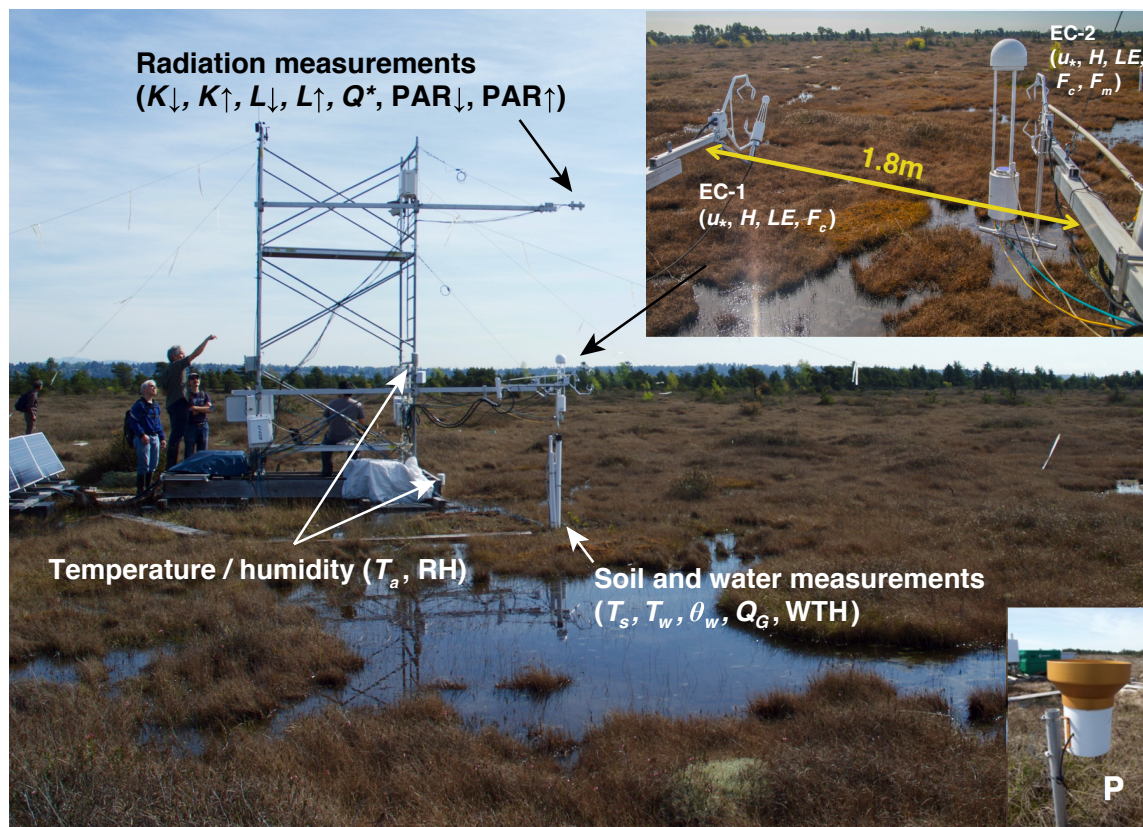


- Minkinen, K. and Laine, J.: Long-term effect of forest drainage on the peat carbon stores of pine mires in Finland, 470 *Canadian Journal of Forest Research*, 28, 1267-1275, 1998.
- Mundava, C.: Mapping vegetation in reconstructed peatlands using spectroscopy for the Haaksbergerveen, s.n.], [S.l., 2011.
- Neter, J., Wasserman, W., and Whitmore, G. A.: *Applied Statistics*, Allyn & Bacon, Newton, Massachusetts, 1988.
- Ögren, E. and Evans, J. R.: Photosynthetic light-response curves, *Planta*, 189, 182-190, 1993.
- Page, S. E., Siegert, F., Rieley, J. O., Boehm, H.-D. V., Jaya, A., and Limin, S.: The amount of carbon released from peat 475 and forest fires in Indonesia during 1997, *Nature*, 420, 61-65, 2002.
- Petrescu, A. M. R., Lohila, A., Tuovinen, J.-P., Baldocchi, D. D., Desai, A. R., Roulet, N. T., Vesala, T., Dolman, A. J., Oechel, W. C., Marcolla, B., Friborg, T., Rinne, J., Matthes, J. H., Merbold, L., Meijide, A., Kiely, G., Sottocornola, M., Sachs, T., Zona, D., Varlagin, A., Lai, D. Y. F., Veenendaal, E., Parmentier, F.-J. W., Skiba, U., Lund, M., Hensen, A., van Huissteden, J., Flanagan, L. B., Shurpali, N. J., Grünwald, T., Humphreys, E. R., Jackowicz-Korczyński, M., Aurela, M. A., 480 Laurila, T., Grüning, C., Corradi, C. A. R., Schrier-Uijl, A. P., Christensen, T. R., Tamstorf, M. P., Mastepanov, M., Martikainen, P. J., Verma, S. B., Bernhofer, C., and Cescatti, A.: The uncertain climate footprint of wetlands under human pressure, *Proceedings of the National Academy of Sciences*, 112, 4594-4599, 2015.
- Pihlatie, M. K., Kiese, R., Brüggemann, N., Butterbach-Bahl, K., Kieloaho, A. J., Laurila, T., Lohila, A., Mammarella, I., Minkinen, K., Penttilä, T., Schönborn, J., and Vesala, T.: Greenhouse gas fluxes in a drained peatland forest during spring 485 frost-thaw event, *Biogeosciences*, 7, 1715-1727, 2010.
- Poindexter, C. M., Baldocchi, D. D., Matthes, J. H., Knox, S. H., and Variano, E. A.: The contribution of an overlooked transport process to a wetland's methane emissions, *Geophysical Research Letters*, 43, 6276-6284, 2016.
- Price, J. S. and Waddington, J. M.: *Advances in Canadian wetland hydrology and biogeochemistry*, Hydrological Processes, 14, 1579-1589, 2000.
- 490 Richards, B. and Craft, C. B.: Greenhouse Gas Fluxes from Restored Agricultural Wetlands and Natural Wetlands, Northwestern Indiana. In: *The Role of Natural and Constructed Wetlands in Nutrient Cycling and Retention on the Landscape*, Vymazal, J. (Ed.), Springer International Publishing, Cham, 2015.
- Rinne, J., Riutta, T., Pihlatie, M., Aurela, M., Haapanala, S., Tuovinen, J.-P., Tuittila, E.-S., and Vesala, T.: Annual cycle of methane emission from a boreal fen measured by the eddy covariance technique, *Tellus B*, 59, 449-457, 2007.
- 495 Rochefort, L., Campeau, S., and Bugnon, J.-L.: Does prolonged flooding prevent or enhance regeneration and growth of *Sphagnum*?, *Aquatic Botany*, 74, 327-341, 2002.
- Schipper, L. A. and Reddy, K. R.: Methane Production and Emissions from Four Reclaimed and Pristine Wetlands of Southeastern United States, *Soil Sci. Soc. Am. J.*, 58, 1270-1275, 1994.
- Schrier-Uijl, A. P., Kroon, P. S., Hendriks, D. M. D., Hensen, A., Van Huissteden, J., Berendse, F., and Veenendaal, E. M.: 500 Agricultural peatlands: towards a greenhouse gas sink &ndash; a synthesis of a Dutch landscape study, *Biogeosciences*, 11, 4559-4576, 2014.





- Schulze, E. D., Lloyd, J., Kelliher, F. M., Wirth, C., Rebmann, C., Lühker, B., Mund, M., Knohl, A., Milyukova, I. M., Schulze, W., Ziegler, W., Varlagin, A. β., Sogachev, A. F., Valentini, R., Dore, S., Grigoriev, S., Kolle, O., Panfyorov, M. I., Tchebakova, N., and Vygodskaya, N. N.: Productivity of forests in the Eurosiberian boreal region and their potential to act as a carbon sink — a synthesis, *Global Change Biology*, 5, 703-722, 1999.
- 505 Shannon, R. and White, J.: A three-year study of controls on methane emissions from two Michigan peatlands, *Biogeochemistry*, 27, 35-60, 1994.
- Shurpali, N. J., HyvÖNen, N. P., Huttunen, J. T., Biasi, C., NykÄNen, H., Pekkarinen, N., and Martikainen, P. J.: Bare soil and reed canary grass ecosystem respiration in peat extraction sites in Eastern Finland, *Tellus B*, 60, 200-209, 2008.
- 510 Shurpali, N. J., Verma, S. B., Kim, J., and Arkebauer, T. J.: Carbon dioxide exchange in a peatland ecosystem, *Journal of Geophysical Research: Atmospheres*, 100, 14319-14326, 1995.
- Strack, M., Waddington, J. M., Rochefort, L., and Tuittila, E. S.: Response of vegetation and net ecosystem carbon dioxide exchange at different peatland microforms following water table drawdown, *Journal of Geophysical Research: Biogeosciences*, 111, n/a-n/a, 2006.
- 515 Strack, M. and Zuback, Y. C. A.: Annual carbon balance of a peatland 10 yr following restoration, *Biogeosciences*, 2013. 12, 2013.
- Tapio-Biström, M. L., Joosten, H., Tol, S., Food, Project, A. O. o. t. U. N. M. o. C. C. i. A., and International, W.: *Peatlands: Guidance for Climate Change Mitigation Through Conservation, Rehabilitation and Sustainable Use*, Food and Agriculture Organization of the United Nations, 2012.
- 520 Tuittila, E.-S., Komulainen, V.-M., Vasander, H., Nykänen, H., Martikainen, P. J., and Laine, J.: Methane dynamics of a restored cut-away peatland, *Global Change Biology*, 6, 569-581, 2000.
- van der Werf, G. R., Randerson, J. T., Collatz, G. J., Giglio, L., Kasibhatla, P. S., Arellano, A. F., Olsen, S. C., and Kasischke, E. S.: Continental-Scale Partitioning of Fire Emissions During the 1997 to 2001 El Niño/La Niña Period, *Science*, 303, 73-76, 2004.
- 525 Waddington, J. M. and Roulet, N. T.: Carbon balance of a boreal patterned peatland, *Global Change Biology*, 6, 87-97, 2000.
- Weltzin, J. F., Pastor, J., Harth, C., Bridgman, S. D., Updegraff, K., and Chapin, C. T.: Response of bog and fen plant communities to warming and water-table manipulations, *Ecology*, 81, 3464-3478, 2000.
- Wilson, D., Farrell, C., Mueller, C., Hepp, S., and Renou-Wilson, F.: Rewetted industrial cutaway peatlands in western Ireland: a prime location for climate change mitigation?, *Mires and Peat*, 11, 2013.
- 530 Yu, Z.: Holocene carbon flux histories of the world's peatlands: Global carbon-cycle implications, *The Holocene*, doi: 10.1177/0959683610386982, 2011. 2011.



535 Figure 1: Flux tower on floating platform with EC-1 and EC-2 systems facing south and instruments that measured climate  
variables indicated (friction velocity ( $u_s$ ), sensible heat flux ( $H$ ), latent heat flux ( $LE$ ),  $\text{CO}_2$  flux ( $F_c$ ),  $\text{CH}_4$  flux ( $F_m$ ),  
incoming shortwave radiation ( $K \downarrow$ ), outgoing shortwave radiation ( $K \uparrow$ ), incoming longwave radiation ( $L \downarrow$ ), outgoing  
longwave radiation ( $L \uparrow$ ), net all-wave radiation ( $Q^*$ ), incoming PAR ( $\text{PAR} \downarrow$ ), outgoing PAR ( $\text{PAR} \uparrow$ ), air temperature ( $T_a$ ),  
relative humidity (RH), soil temperature ( $T_s$ ), water temperature ( $T_w$ ), soil water content ( $\theta_w$ ), soil heat flux ( $Q_G$ ), water table  
540 height (WTH), and precipitation (P)).

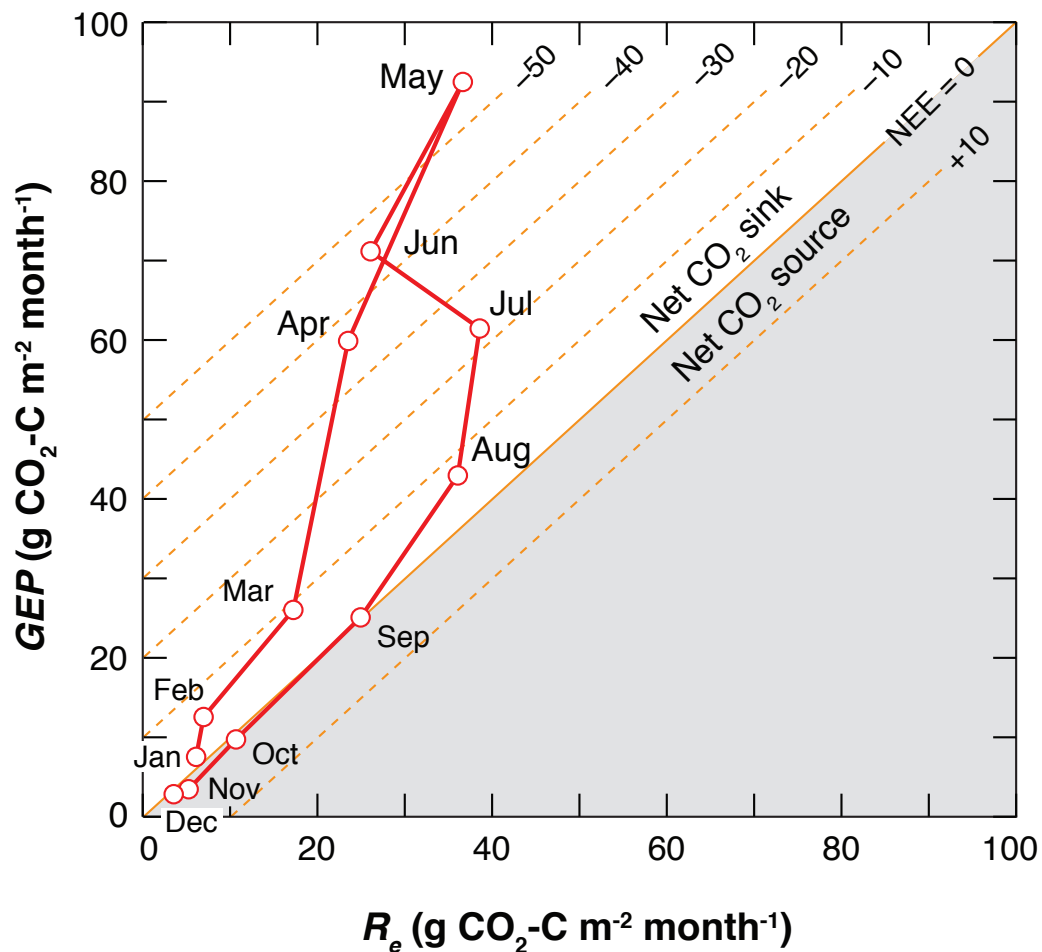
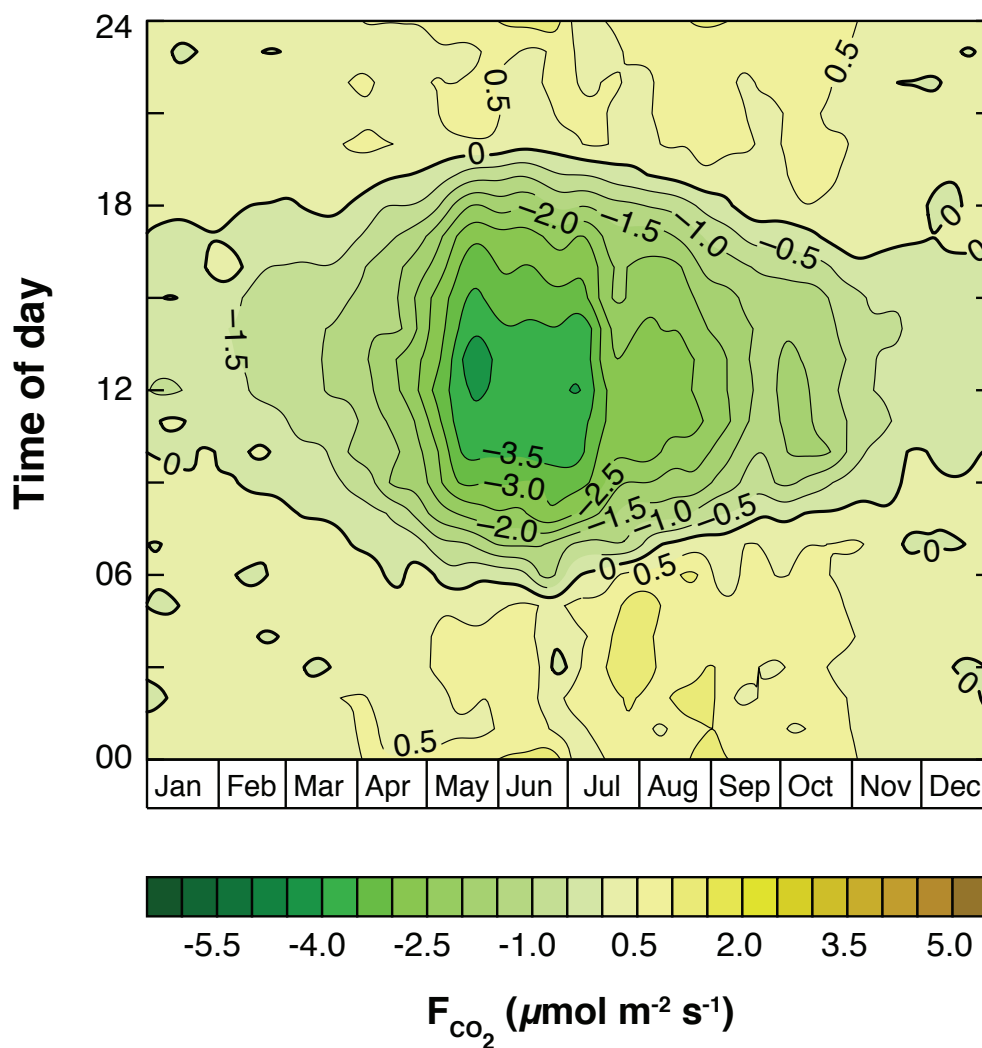


Figure 2: Monthly gap-filled  $R_e$  (x-axis) drawn against GEP (y-axis). The resulting NEE can be read off the diagonal lines. The thick 1:1 line shows carbon neutrality, while lines in the upper right are of increasingly negative NEE (uptake) and lines towards the lower right are positive NEE (net source).



545

Figure 3: Isoleths of gap-filled NEE (net CO<sub>2</sub> fluxes) from the EC-1 system plotted as a composite in the study year. The graph uses a Gaussian filter of  $\sigma = 45$  days (which conserves total NEE) to graphically smooth horizontal variations.

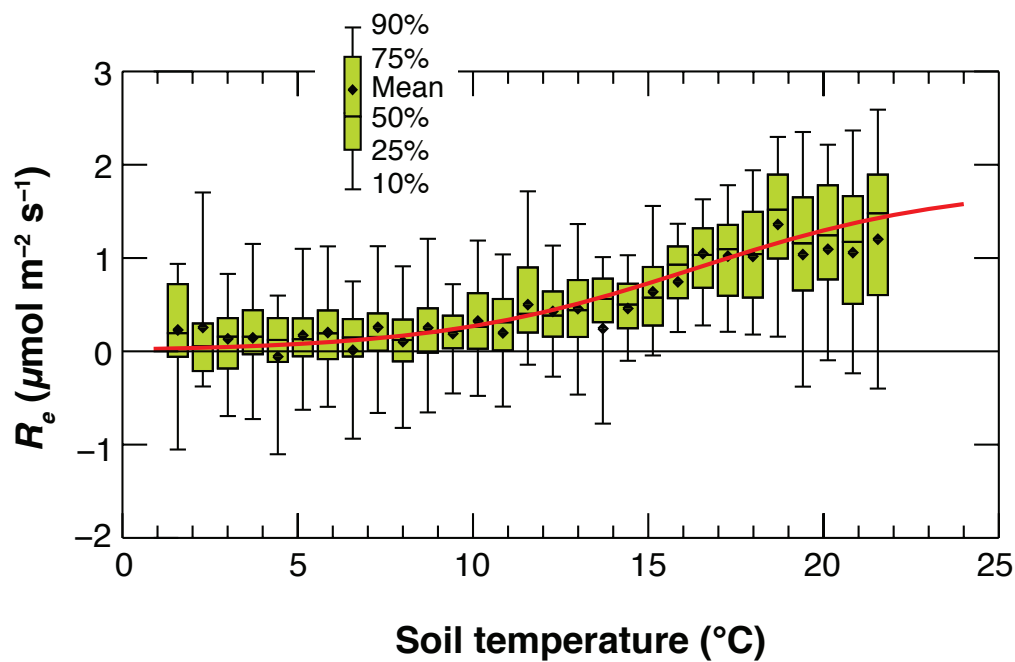
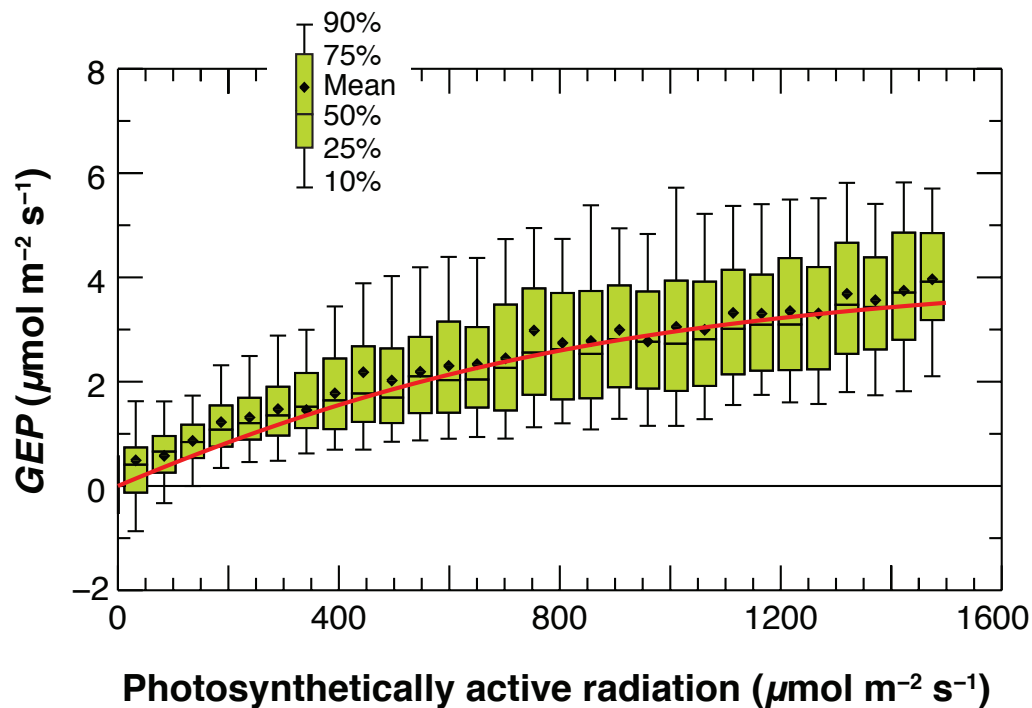
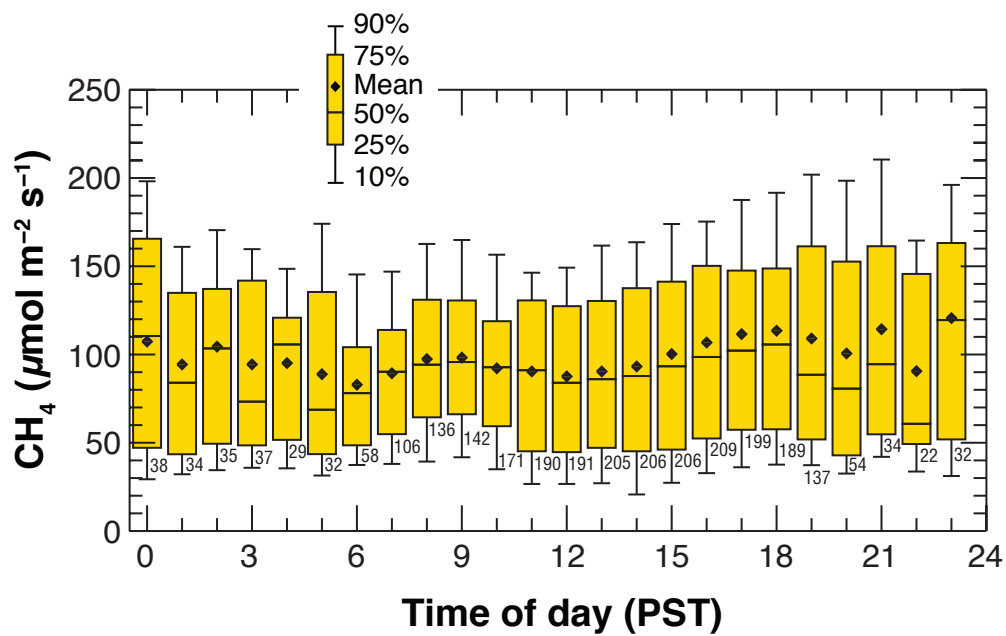


Figure 4: Relationship between  $R_e$  (nighttime 30-minute  $\text{CO}_2$  flux measurements) and  $T_{s,5cm}$  during the entire study period. The  $u_*$  threshold was  $0.08 \text{ m s}^{-1}$ . The fitted curve is a logistic relationship following Eq. 1.  $T_{s,5cm}$  was binned for 32 classes from minimum of  $T_{s,5cm}$  to maximum of  $T_{s,5cm}$ . See Fig. S3 in supplement for seasonal differences. Negative  $R_e$  values were caused by measurement uncertainties.



555 Figure 5: Annual light response curve determined from the daytime 30-minute NEE measurements and Eq. 1, i.e.,  $GEP = R_c + \text{-NEE}$ . The curves are the best fit of the Eq. 2. PPFD was binned for 30 classes from 0 to  $1500 \mu\text{mol m}^{-2} \text{s}^{-1}$ . Annual  $MQY$  was  $4.00 \text{ mmol C mol}^{-1} \text{ photons}$ ,  $P_M$  was  $4.68 \mu\text{mol m}^{-2} \text{s}^{-1}$ , and  $C_v$  was 0.7 (fixed).



560

Figure 6: (a) Diurnal course of filled  $\text{CH}_4$  fluxes from the EC-2 system in the entire study period.

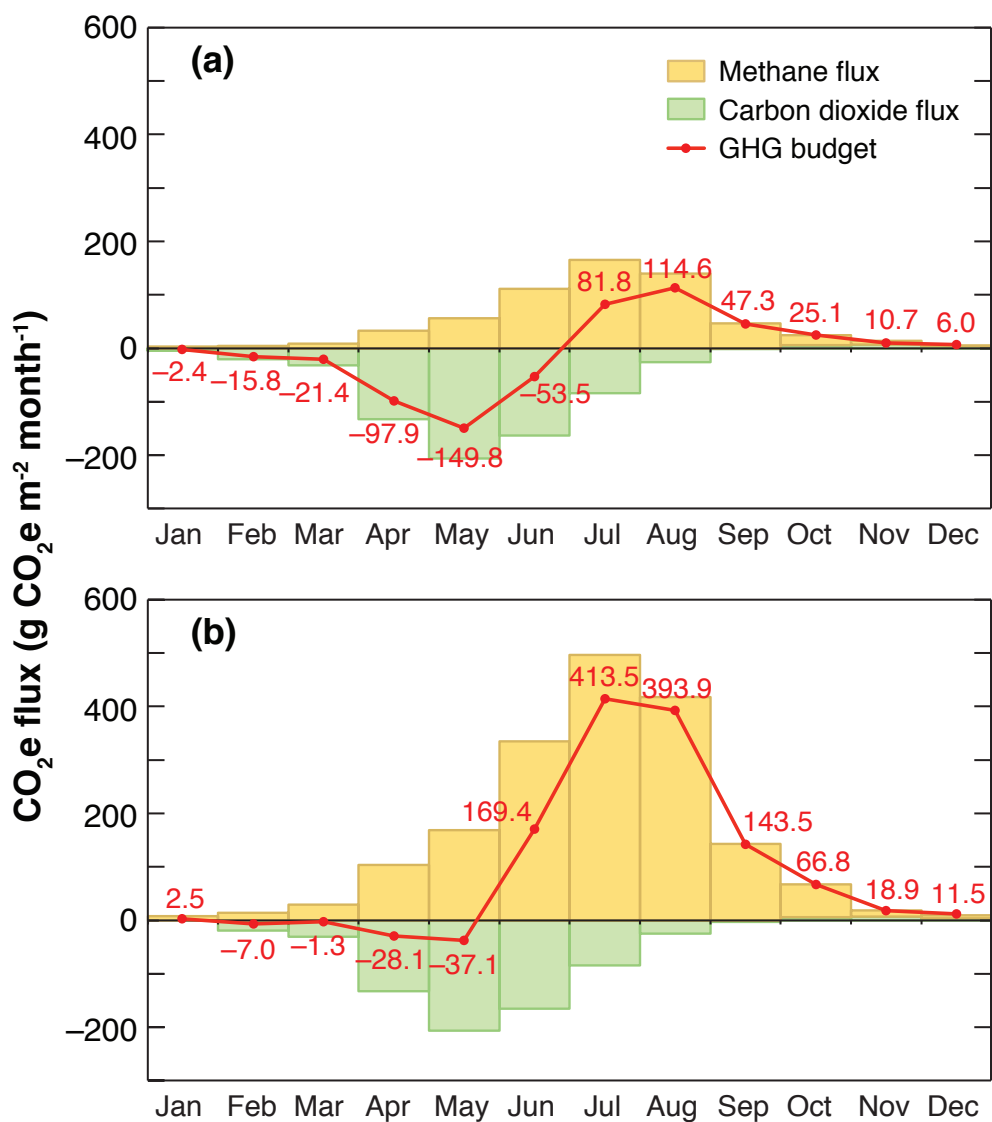


Figure 7: EC-measured monthly CO<sub>2</sub>, CH<sub>4</sub> and net GHGs fluxes shown as CO<sub>2</sub>e totals by using (a) 100-year and (b) 20-year GWPs. Missing data were gap-filled.




 565 Table 1: Monthly EC-measured and gap-filled NEE (CO<sub>2</sub> fluxes), CH<sub>4</sub> fluxes, CO<sub>2</sub>e fluxes using 20-year GWP, and CO<sub>2</sub>e fluxes using 100-year GWP at the study site during the study period.

Month	<i>R<sub>e</sub></i>	GEP	NEE	CH <sub>4</sub> fluxes (mg CH <sub>4</sub> -C m <sup>-2</sup> month <sup>-1</sup> )	20-year CO <sub>2</sub> e fluxes (g CO <sub>2</sub> e m <sup>-2</sup> month <sup>-1</sup> )	100-year CO <sub>2</sub> e fluxes (g CO <sub>2</sub> e m <sup>-2</sup> month <sup>-1</sup> )
	(g CO <sub>2</sub> -C m <sup>-2</sup> month <sup>-1</sup> )					
Jan	6.17	7.50	-1.33	66	2.5	-2.4
Feb	6.94	12.46	-5.52	118	-7.0	-15.8
Mar	17.33	25.89	-8.59	269	-1.3	-21.4
Apr	23.52	59.73	-36.21	933	-28.0	-97.8
May	36.46	92.63	-56.20	1506	-37.0	-149.6
Jun	26.13	71.10	-44.97	2980	169.5	-53.3
Jul	38.53	61.47	-22.94	4436	413.6	81.8
Aug	36.15	42.97	-6.82	3734	393.9	114.6
Sep	24.84	25.08	-0.21	1286	143.5	47.3
Oct	10.76	9.58	1.18	557	66.8	25.2
Nov	5.16	3.39	1.77	111	18.9	10.6
Dec	3.63	2.79	0.87	74	11.5	6.0
Study year	g CO <sub>2</sub> -C m <sup>-2</sup> year <sup>-1</sup>			g CH <sub>4</sub> -C m <sup>-2</sup> year <sup>-1</sup>	g CO <sub>2</sub> e m <sup>-2</sup> year <sup>-1</sup>	
	236	415	-179	16	1147	-55



570 Table 2: Comparison of annual NEE,  $R_e$  and GEP, over different ecosystems (vegetation covers) in the Vancouver region using EC measurements. Sorted by magnitude of -NEE/GEP ratio.

Site	Land cover	NEE	$R_e$	GEP	-NEE/GEP
		g C m <sup>-2</sup> year <sup>-1</sup>			
<b>Burns Bog (this study)</b> Delta, BC	Rewetted raised bog ecosystem	-179	236	415	43%
<b>Westham Island (CA-Wes)*</b> Delta, BC	Unmanaged grassland	-222	1215	1438	15%
<b>Campbell River (CA-Ca1)*</b> Vancouver Island	Douglas-fir forest (~55 yrs)	-328 <sup>+</sup>	1830 <sup>+</sup>	2158 <sup>+</sup>	15%
<b>Buckley Bay (CA-Ca3)*</b> Vancouver Island	Douglas-fir forest (~15 yrs)	64 <sup>+</sup>	1487 <sup>+</sup>	1423 <sup>+</sup>	-4%

\* Site identifier in global FLUXNET database (<http://fluxnet.ornl.gov>).

<sup>+</sup> Data from Krishnan et al., 2009 before fertilisation.

575